Computing Halo Orbits: A Reconstruction of the ISEE-3 Mission Orbit

Sai Chikine
ASEN 5050 Research Project 2017

The circular restricted three body problem is a well known model in astrodynamics wherein two large primaries are assumed to be moving in circular orbits, while the third body, whose mass is negligible compared to the primaries, is influenced by their combined gravity but does not influence them in turn. In this model, there exist five equilibrium points in the system, called libration points. Three of these are collinear, and can support unstable periodic orbits around them. In this project, a halo orbit, which is a periodic orbit with out of plane components, around Sun-Earth L1 is constructed. Specifically, the orbit of ISEE-3, which was the first satellite mission to implement a halo orbit, is replicated and validated against known parameters. A third order analytical approximation is used to construct a rough halo orbit which is then adjusted to a periodic orbit using differential correction.

I. Introduction

Halo orbits are an extremely useful mission design tool in that they allow for placement of spacecraft in ideal positions to accomplish some science goals. For instance, a spacecraft placed in an L2 orbit in the Earth-Moon system would appear, from the Earth, to follow a 'halo' around the Moon[1]. Arthur C. Clarke suggested such an orbit could enable constant communication with a colony on the far side of the Moon. Another application of this type of orbit is the James Webb space telescope. JWST will orbit Sun-Earth L2, located on the far side of the Earth, shielding the telescope from the Sun and allow it to remain relatively stationary relative to Earth, enabling easy communication. This project is concerned with the International Sun-Earth Explorer-3 (ISEE-3) mission, which used a halo orbit that allowed for constant monitoring of the Sun. If it had been in an Earth centered elliptical orbit instead, the Sun would be obscured by the Earth for at least some of its orbit, wasting valuable mission time.

A. ISEE-3 Mission Background

ISEE-3 was part of the International Sun-Earth Explorer mission program, which utilized three spacecraft. The mission goals were: "(1) to investigate solar-terrestrial relationships at the outermost boundaries of the Earth's magnetosphere; (2) to examine in detail the structure of the solar wind near the Earth and the shock wave that forms the interface between the solar wind and Earth's magnetosphere; (3) to investigate motions of and mechanisms operating in the plasma sheets; and, (4) to continue the investigation of cosmic rays and solar flare emissions in the interplanetary region near 1 AU," ([2]). To this end, it was placed in an orbit around Sun-Earth L1. This point lies directly between the Sun and the Earth, making it an ideal spot to place a spacecraft studying the Sun. In this position, ISEE-3 was able to keep the Sun in view at all times during its orbit, and transmit data to Earth relatively quickly. Although halo orbits were known to exist for several centuries, ISEE-3 was the first spacecraft to actually use one, proving their viability.

II. Circular Restricted Three Body Problem

The model used to develop and compute halo orbits is called the circular restricted three body problem (CR3BP). The three bodies in this situation are the Sun (m_1), the Earth (m_2), and the spacecraft (m_3). When developing this model, the following assumptions are made:

- The spacecraft is treated as a *test particle* moving in the vicinity of the two primaries ($m_3 << m_1, m_2$).
- The two primaries move in circular orbits about their mutual barycenter.
- The spacecraft does not affect the motion of the two primaries.

With these assumptions in place, the equations of motion for the spacecraft can be built. These equations will be in normalized (nondimensional) units, where the following conversions are used [3]. Note that the normalized system is

unprimed and the dimensionalized system is primed.

$$\text{distance } d' = Ld$$
$$\text{velocity } s' = Vs$$
$$\text{time } t' = \frac{T}{2\pi}t$$

and where $L = ||\overrightarrow{r}_{12}||$ (the distance between the two primaries), V is the orbital velocity of the first primary, and T is the orbital period of the primaries. Furthermore, mass is normalized using the mass parameter μ:

$$\mu = \frac{m_2}{m_1 + m_2}$$

Now, the normalized masses of the primaries are:

$$\mu_1 = 1 - \mu$$
$$\mu_2 = \mu$$

And, in the normalized, rotating frame:

$$\text{Distance between primaries} = 1$$
$$m_1 \text{ position} = (-\mu, 0, 0)$$
$$m_2 \text{ position} = (1 - \mu, 0, 0)$$
$$G = 1$$
$$\text{Orbit period of primaries} = 2\pi$$

In an inertial frame, the acceleration of the spacecraft is expressed as:

$$\overrightarrow{\ddot{R}_{s/c}}^I = -\frac{1-\mu}{R_1^3}\overrightarrow{R_1} - \frac{\mu}{R_2^3}\overrightarrow{R_2} \tag{1}$$

From here, we will switch to a rotating frame which rotates with the primaries such that the x-axis is always along the line connecting them. This frame is referred to as the synodic frame. Converting this vector equation to the synodic frame and to a scalar form results in the following equations of motion [4]:

$$\ddot{x} = 2\dot{y} + x - (1-\mu)\frac{x+\mu}{r_1^3} - \mu\frac{x-1-\mu}{R_2^3} \tag{2}$$
$$\ddot{y} = -2\dot{x} + y - (1-\mu)\frac{y}{R_1^3} - \mu\frac{y}{R_2^3} \tag{3}$$
$$\ddot{z} = -(1-\mu)\frac{z}{R_1^3} - \mu\frac{z}{R_2^3} \tag{4}$$

where R_1 and R_2 are the distances from the spacecraft to the first and second primaries, respectively, and are given as:

$$R_1^2 = (x+\mu)^2 + y^2 + z^2 \tag{5}$$
$$R_2^2 = (x-1-\mu)^2 + y^2 + z^2 \tag{6}$$

III. Libration Points

The gravitational potential in the CR3BP can be expressed as [3]

$$U(x, y, z) = -\frac{\mu_1}{R_1} - \frac{\mu_2}{R_2} - \frac{1}{2}\mu_1\mu_2 \tag{7}$$

We can then write the *effective potential* in the synodic frame, which includes rotational effects, as

$$\bar{U}(x, y) = -\frac{1}{2}(\mu_1 R_1^2 + \mu_2 R_2^2) - \frac{\mu_1}{R_1} - \frac{\mu_2}{R_2} \tag{8}$$

A sample of this potential is plotted in Figure 1[3]. In this figure, we can see the three **collinear** libration points: L_1, L_2, L_3, which lie along the x-axis in the synodic frame. The large gap in the figure is the gravity well created by the first primary (the Sun in this case), while the smaller gap is the gravity well created by the second primary (Earth in this case).
Figure 2 shows the libration points projected onto the $x - y$ plane (in the synodic frame) [3]. These locations are *equilibrium* points, where the net gravitational force is zero.

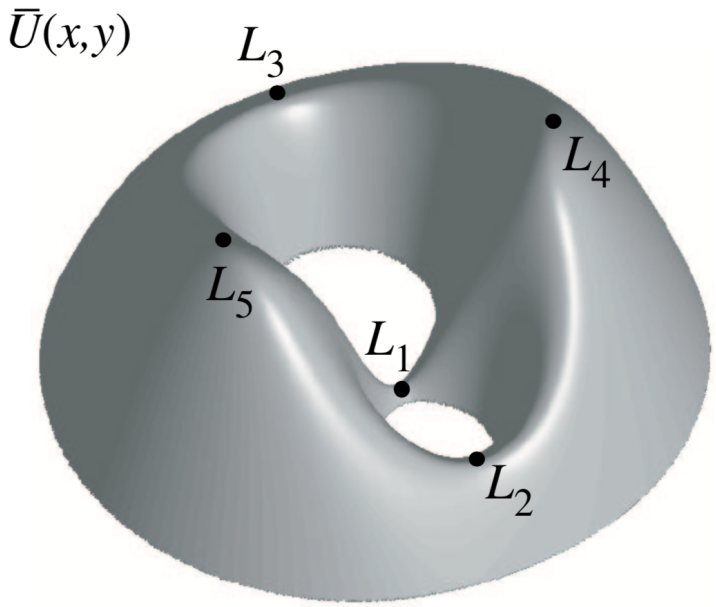

Fig. 1 (Courtesy of Koon, Lo, Marsden, Ross) Plot of the effective potential for $\mu = 0.3$. The marked points are the libration points, and are critical points of the potential function.

IV. Halo Orbits

To begin studying halo orbits, we will linearize the equations of motion around the collinear libration points. In this formulation, which follows Koon, Lo, Marsden, and Ross' treatment [3], a coordinate change must be implemented first:

$$\bar{x} = \frac{x - 1 + \mu + \gamma}{\gamma} \tag{9}$$

$$\bar{y} = \frac{y}{\gamma} \tag{10}$$

$$\bar{z} = \frac{z}{\gamma} \tag{11}$$

where γ is the distance from the second primary (Earth) to the L1 point, in this case.

Then, the nonlinear parts of the equations of motion are separated and expanded using Legendre polynomials. Doing so results in

$$\ddot{x} - 2\dot{y} - (1 + 2c_2)x = 0 \tag{12}$$

$$\ddot{y} + 2\dot{x} + (c_2 - 1)y = 0 \tag{13}$$

$$\ddot{z} + c_2 z = 0 \tag{14}$$

where the coefficients c_n are

$$c_n = \frac{1}{\gamma^3}(1^n\mu + (-1)^n \frac{(1-\mu)\gamma^{n+1}}{(1-\gamma)^{n+1}}) \tag{15}$$

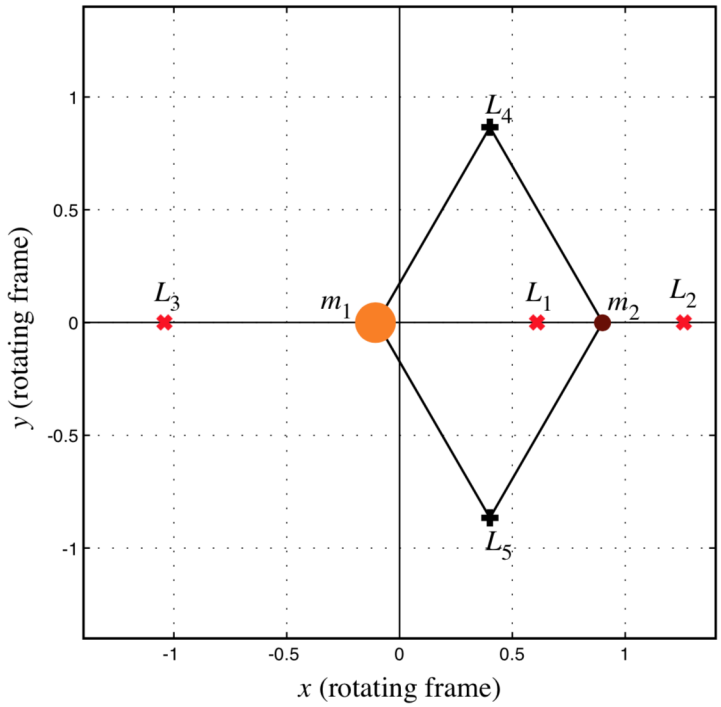

Fig. 2 (Courtesy of Koon, Lo, Marsden, Ross) Libration (equilibrium) points in the $x - y$ plane.

and come from the Legendre polynomial terms.

This system yields eigenvalues of $\pm\lambda, \pm i\omega_p, \pm\omega_v$, which are given by:

$$\lambda^2 = \frac{c_2 + \sqrt{9c_2^2 - 8c_2}}{2} \tag{16}$$

$$\omega_p^2 = \frac{2 - c_2 + \sqrt{9c_2^2 - 8c_2}}{2} \tag{17}$$

$$\omega_v^2 = c_2 \tag{18}$$

When only bounded solutions are chosen, the above equations have solutions:

$$x = -A_x \cos(\omega_p t + \phi) \tag{19}$$

$$y = \kappa A_x \sin(\omega_p t + \phi) \tag{20}$$

$$z = A_z \sin(\omega_v t + \psi) \tag{21}$$

We can see that the x and y motions are coupled through their frequency ω_p, as well as the constant κ, which is defined by:

$$\kappa = \frac{\omega_p^2 + 1 + 2c_2}{2\omega_p} \tag{22}$$

Furthermore, for halo orbits, the amplitudes A_x and A_z are also constrained via the equation:

$$l_1 A_x^2 + l_2 A_z^2 + \Delta = 0 \tag{23}$$

where l_1, l_2, and Δ are constants defined by the coefficients c_n.

Halo orbits are periodic, and are characterized by having equal eigenfrequencies ($\omega_p = \omega_v$). So, as a first order linear approximation of a halo orbit, we have the following equations:

$$x = -A_x \cos(\omega_p t + \phi) \tag{24}$$
$$y = \kappa A_x \sin(\omega_p t + \phi) \tag{25}$$
$$z = A_z \sin(\omega_p t + \psi) \tag{26}$$

Note that A_z may be negative, as well. The difference between the positive and negative z amplitudes is characterized via *northern* and *southern* halo orbits. Northern halo orbits have a maximum out of plane component above the xy-plane, while southern halo orbits have a maximum out of plane component below the xy-plane. In this case, ISEE-3's orbit is a southern halo orbit.

From here, the **Lindstedt-Poincare** method is used to construct successive approximations based on this linear approximation. This method essentially removes secular terms that cause solutions to blow up. In this case, a third order approximation (Richardson extrapolation) is used, which is given by:

$$x = a_{21}A_x^2 + a_{22}A_z^2 - A_x \cos t + (a_{23}A_x^2 - a_{24}A_z^2)\cos(2t) + (a_{31}A_x^3 - a_{32}A_x A_z^2 - a_{24}A_z^2)\cos(3t) \tag{27}$$
$$y = \kappa A_x \sin t + (b_{21}A_x^2 - b_{22}A_z^2)\sin(2t) + (b_{31}A_x^3 - b_{32}A_x A_z^2)\sin(3t) \tag{28}$$
$$z = \delta_m(A_z \cos(t) + d_{21}A_x A_z(\cos(2t) - 3) + (d_{32}A_z A_x^2 - d_{31}A_z^3)\cos(3t)) \tag{29}$$

The δ_m in the z solution is either $+1$ or -1, based on whether the halo orbit is a northern or southern halo orbit, respectively, so $\delta_m = -1$ in our case.

The period of the third order approximate halo orbit can be found using a frequency connection term ν introduced during the process of the Lindstedt-Poincare method, and is given by

$$T = \frac{2\pi}{\omega_p \nu},\ \nu = 1 + \nu_1 + \nu_2, \tag{30}$$
$$\nu_1 = 0 \tag{31}$$
$$\nu_2 = s_1 A_x^2 + s_2 A_z^2 \tag{32}$$

The coefficients a_{ij}, b_{ij}, d_{ij}, and $s_{1,2}$ are all functions of the c_n coefficients, and are detailed in Koon, Lo, Marsden, and Ross [3].

V. Computing Halo Orbits: Differential Correction

By using the third order solution and setting $t = 0$, initial conditions can be found for an third order approximation of a halo orbit. However, numerically integrating from this initial state vector reveals that this approximation breaks down quickly (less than one orbit period), as shown in Figures 3 and 4.

Since even this high order approximation breaks down quickly, we will use a numerical method to compute better initial conditions for a halo orbit that is actually periodic.

Broadly, we start with some set of initial conditions and evaluate whether they will result in a periodic orbit. If not, we adjust them accordingly and try again. However, trajectories around L1 are very sensitive to initial conditions, and a starting guess which is not close to our true halo orbit will not result in convergence. This is where the third order approximation becomes beneficial: using the initial conditions computed from our third order approximation will result in rapid convergence to the desired initial conditions.

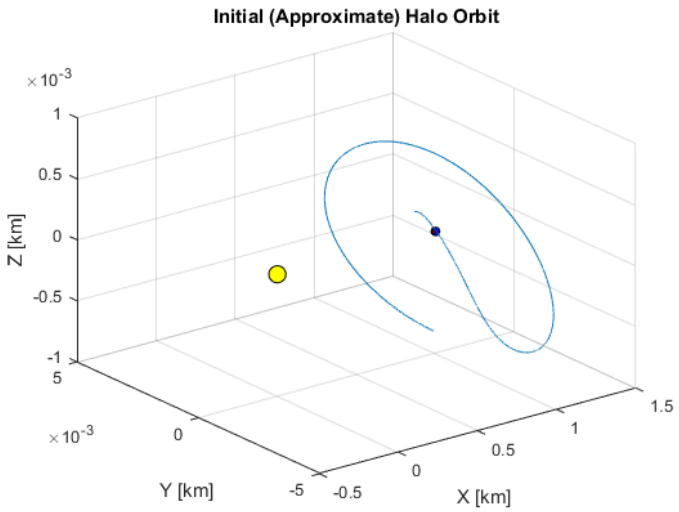

Fig. 3 Orbit propagated using third order initial conditions. The orbit starts from below the xy plane. It quickly diverges from our desired trajectory and is clearly non periodic.

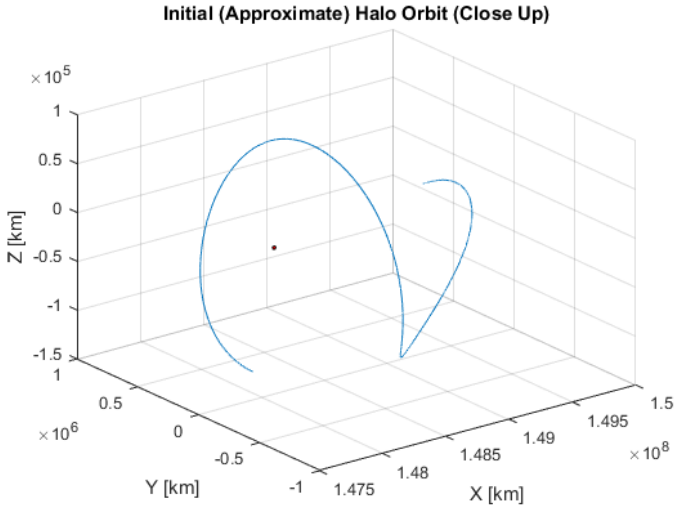

Fig. 4 Local view of orbit propagated using third order initial conditions. The small dot indicates the L1 point.

A. Differential Correction Overview

The process of iteration used here is called **differential correction**. Following Koon, Lo, Marsden, and Ross' treatment [3], we begin with $\phi(t, t_0)$, which represents the trajectories of a system from t_0 to t. Let $\bar{x}(t)$ represent a reference trajectory. Then, an initially perturbed trajectory, with initial conditions $\bar{x}_0 + \delta\bar{x}_0$, will have a final displacement at time t_1 of:

$$\delta\bar{x}(t_1) = \phi(t_1; \bar{x}_0 + \delta\bar{x}_0) - \phi(t_1; \bar{x}_0) \tag{33}$$

We then expand the right side with a Taylor series, which gives us

$$\delta\bar{x}(t_1) = \frac{\partial\phi(t_1; \bar{x}_0)}{\partial x_0}\delta\bar{x}_0 + \text{HOTs} \tag{34}$$

The partial derivative matrix in the above equation is called the state transition matrix (STM), denoted by Φ, and tells us how perturbations in initial conditions translate to perturbations at time t w.r.t. the reference trajectory.

Now, if we have initial conditions $\bar{x}_0$ and a target x_d at time t_1, we have (assuming x_d is not reached):

$$\bar{x}(t_1) = \phi(t_1, t_0; \bar{x}_0) = \bar{x}_1 = x_d - \delta\bar{x}_1$$

We can see that we are a distance $\delta\bar{x}_1$ away from our goal. We can write:

$$\begin{aligned}
\phi(t_1, t_0; \bar{x}_0 + \delta\bar{x}_0) &= \phi(t_1, t_0; \bar{x}_0) + \frac{\partial\phi(t_1; \bar{x}_0)}{\partial x_0}\delta\bar{x}_0 + \text{HOTs} \\
&= \phi(t_1, t_0; \bar{x}_0) + \Phi(t_1, t_0)\delta\bar{x}_0 + \text{HOTs} \\
&= \bar{x}_1 + \delta\bar{x}_1 + \text{HOTs} \\
&= x_d + \text{HOTs}
\end{aligned}$$

So changing the initial conditions by $\delta\bar{x}_0$ gets us to our goal x_d to a first order approximation. As such, we must iteratively apply this until we are within some small ϵ bound of our target.

Since Φ gave us the relationship between $\delta\bar{x}_0$ and $\delta\bar{x}_1$, we can easily solve for our needed correction $\delta\bar{x}_0$:

$$\delta\bar{x}_0 = \Phi(t_1, t_0)^{-1}\delta\bar{x}_1 \tag{35}$$

Now, all that is left is calculating our state transition matrix. The STM can be shown to solve the initial value problem:

$$\begin{gathered}
\dot{\Phi}(t, t_0) = Df(\bar{x}(t))\Phi(t, t_0) \\
\text{where } \Phi(t_0, t_0) = I_n
\end{gathered}$$

where f represents the system dynamics according to $\dot{x} = f(x)$. In general, the above equation for Φ needs to be numerically integrated.

Generally, the technique of differential corrections is extremely useful as it allows for arbitrarily targeting trajectories with specified goals. For example, this method could also be applied to designing Lyapunov orbits, which are in-plane orbits around libration points, as well as transfers to and from libration orbits.

B. Differential Correction: Halo Orbits

In this case, our system dynamics model f is just the scalar equations of motion for the CR3BP written as a system of first order DEs [5]. We will be numerically integrating

$$\dot{\bar{x}} = f(\bar{x}) \tag{36}$$

$$\dot{\Phi}(t, t_0) = Df(\bar{x})\Phi(t, t_0) \tag{37}$$

The first part of the system has 6 ODEs, while the second part has 36 (one for each component of $Df(\bar{x})$. This Jacobian matrix is

$$Df(\bar{x}) = \begin{bmatrix} 0_3 & I_3 \\ \frac{\partial \bar{g}}{\partial \bar{r}} & \frac{\partial \bar{g}}{\partial \bar{v}} \end{bmatrix} \tag{38}$$

$$\text{where } \bar{g} = \begin{bmatrix} \ddot{x} \\ \ddot{y} \\ \ddot{z} \end{bmatrix} \tag{39}$$

Since we know halo orbits are symmetric about the xz-plane, and the trajectory is normal to this plane when it crosses, we can write our initial conditions in the form

$$\bar{x}_{\text{approx}} = (x_0, 0, z_0, 0, \dot{y}_0)^T$$

This guess comes from the third order approximation, where we set $t = 0$. We also know that the next time the trajectory pierces the xz-plane (half an orbit period) where it will be at x_f, it should have a similar form, with the zero components maintained at zero. However, $\dot{x}_f$ and $\dot{z}_f$ will probably be nonzero the first time a crossing occurs, and we wish to drive them to zero with differential correction. We cannot change our zero components, so we vary x_0, z_0, and $\dot{y}_0$.

In this case, since we are aiming for a halo orbit with a desired A_z, and at $t = 0$, we are at the 'bottom' of the halo orbit, we can safely assume that our third order approximation correctly captured z_0. Therefore, we restrict the differential correction algorithm to only being able to vary x_0 and $\dot{y}_0$. Now, we only have to invert a 2x2 matrix (only those components affecting x_0 and $\dot{y}_0$) every iteration. The reduced complexity 2x2 update equation is [6]:

$$\begin{bmatrix} \delta\dot{x} \\ \delta\dot{z} \end{bmatrix} = \left[\begin{pmatrix} \Phi_{41} & \Phi_{45} \\ \Phi_{61} & \Phi_{65} \end{pmatrix} - \tfrac{1}{\dot{y}} \begin{pmatrix} \ddot{x} \\ \ddot{z} \end{pmatrix} \begin{pmatrix} \Phi_{21} & \Phi_{25} \end{pmatrix} \right] \begin{bmatrix} \delta x_0 \\ \delta\dot{y}_0 \end{bmatrix} \tag{40}$$

$$\therefore \begin{bmatrix} \delta x_0 \\ \delta\dot{y}_0 \end{bmatrix} = \left[\begin{pmatrix} \Phi_{41} & \Phi_{45} \\ \Phi_{61} & \Phi_{65} \end{pmatrix} - \tfrac{1}{\dot{y}} \begin{pmatrix} \ddot{x} \\ \ddot{z} \end{pmatrix} \begin{pmatrix} \Phi_{21} & \Phi_{25} \end{pmatrix} \right]^{-1} \begin{bmatrix} \delta\dot{x} \\ \delta\dot{z} \end{bmatrix} \tag{41}$$

We continue to iterate until $\dot{x}_f = \dot{z}_f = 0$ at the xz-plane crossing.

In practice, this stopping condition is equivalent to the magnitude of the correction vector $\left[\delta x_0; \delta\dot{y}_0\right]^T$ reaching zero; as the conditions get closer and closer to the desired state, our corrections also vanish. Additionally, instead of relying on the third order approximation for the orbit period, we can set our ODE solver to stop integrating when $y = 0$, signaling an xz-plane crossing.

VI. Implementation and Results

Koon, Lo, Marsden, and Ross specify the information necessary to compute all needed constants for the ISEE-3 orbit. Sun-Earth eigenvalues are provided, which, when combined with the ISEE-3 orbit parameters, are enough to define the system. The ISEE-3 orbit is specified to the following orbit parameters [3]:

$$A_x = 206,000\ km$$
$$A_y = 665,000\ km$$
$$A_z = 110,000\ km$$
$$T = 177.73 \text{ days}$$

Halo orbits are uniquely determined by their A_z amplitude, so all other parameters are calculated from this value. From the third order approximation, the initial guess used (in the γ normalized system) was:

$$\bar{x}_{0,\text{guess}} = \begin{bmatrix} 0.98887524 & 0 & -8.10869349 \times 10^{-4} & 0 & 0.00903870 & 0 \end{bmatrix}^T$$

The calculated period using $T = \frac{2\pi}{\omega_p \nu}$ was 177.587 days. A convergence bound of $1e-13$ was used, and the algorithm converged in 5 iterations. Afterwards, the updated initial conditions were:

$$\bar{x}_{0,\text{converged}} = \begin{bmatrix} 0.98888234 & 0 & -8.10869349 \times 10^{-4} & 0 & 0.00890416 & 0 \end{bmatrix}^T$$

According to the ODE solver, the half period time (time until $y = 0$) was 88.8729 days (after conversion back to dimensionalized units). This means the total period after convergence was 177.746 days, which is very close to the reported value of 177.73 days.

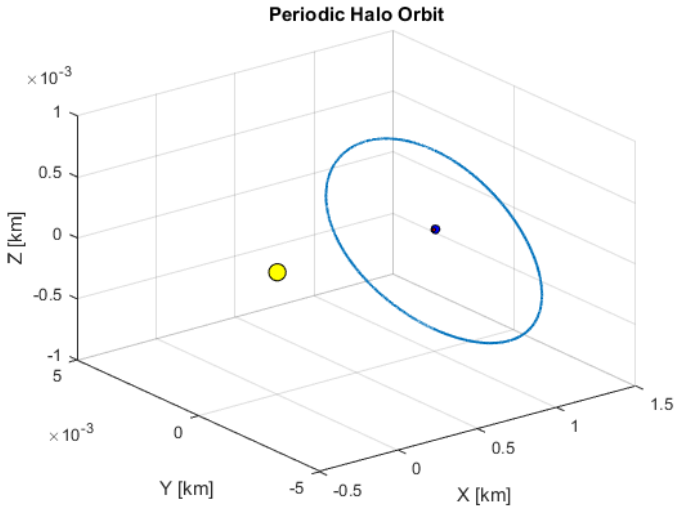

Fig. 5 Halo orbit propagated using finalized initial conditions. The orbit is closed and periodic.

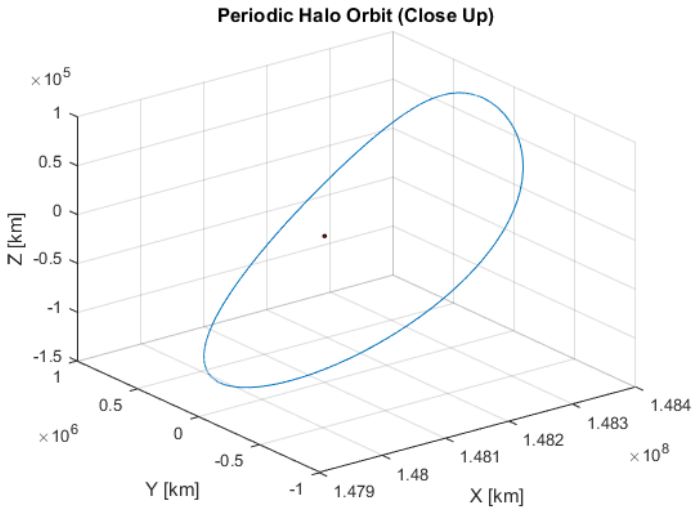

Fig. 6 Local view of finalized orbit. The small dot indicates the L1 point.

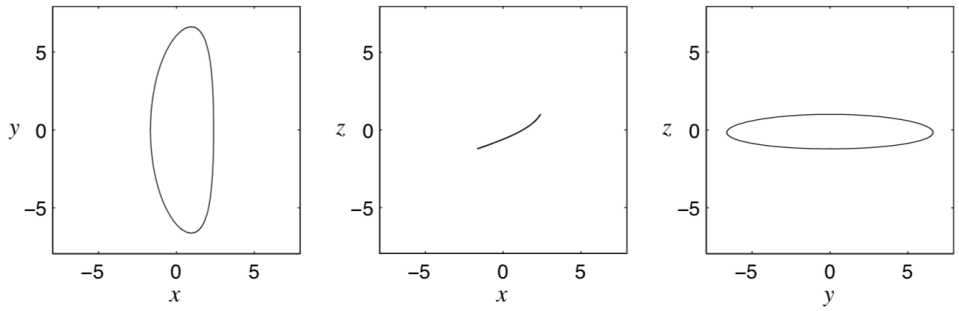

Fig. 7 (Courtesy of Koon, Lo, Marsden, and Ross) ISEE-3 halo orbit, projected onto the indicated planes. Units are normalized by 10^5 km.

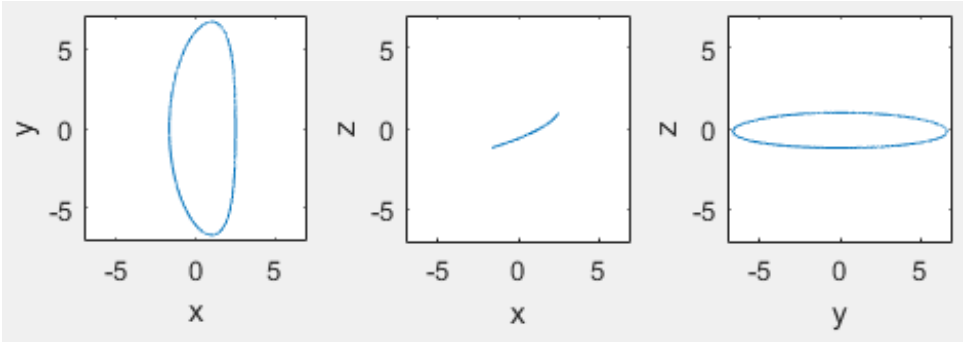

Fig. 8 Simulated ISEE-3 halo orbit, projected onto the indicated planes. Units are normalized by 10^5 km.

The halo orbit propagated for one full period after convergence is shown in Figures 5 and 6. We can see that the orbit is periodic and no longer diverges. Furthermore, the final reported amplitudes after convergence were:

$$A_x = 207,530\ km$$
$$A_y = 665,580\ km$$
$$A_z = 109,410\ km$$

These values also agree well with the historical values, with the maximum deviation being 0.74%.

Figure 7 shows ISEE-3's halo orbit projected onto 3 perpendicular planes, taken from Koon, Lo, Marsden, and Ross [3]. Figure 8 shows the orbit computed in this simulation in the same three projections.

Overall, based on agreement with the literature concerning ISEE-3's orbit, this simulation was fairly successful in replicating the historic mission orbit.

VII. Summary and Conclusions

This project used the circular restricted three body problem combined with the method of differential correction to replicate the ISEE-3 halo orbit. The computed orbit amplitudes, as well as the period, agree well with the reference values taken from Koon, Lo, Marsden, and Ross, and validate the approach used here. The project demonstrates the power of using differential corrections to create a target orbit. Since ISEE-3, many spacecraft have used halo orbits, including GENESIS and DSCOVR. Undoubtedly, halo orbits will continue to be a valuable tool to astrodynamicists and trajectory designers. Their ability to place spacecraft in positions ideally suited for science goals means they are essential to modern astrodynamics.

This project can serve as a jumping off point to a few more in depth analyses. One example would be modeling 4 body effects on halo orbits; a halo orbit around Sun-Earth L2 could be significantly impacted by the Moon's influence. Another direction would be to design a transfer into or out of this halo orbit. ISEE-3 was eventually moved out of its halo orbit to study a comet. Understanding and/or modeling this maneuver's design would be extremely insightful.

References

[1] Farquhar, R., "Halo-orbit and Lunary-swingby Missions of the 1990s," *Acta Astronautica*, Vol. 24, 1994, pp. 227–234.

[2] "NASA ISEE-3 Mission Page," `https://nssdc.gsfc.nasa.gov/nmc/spacecraftDisplay.do?id=1978-079A`, 2017. Accessed: 12/13/17.

[3] Koon, W. S., Lo, M. W., Marsden, J. E., and Ross, S. D., *Dynamical Systems, The Three-Body Problem, and Space Mission Design*, 2006.

[4] Davis, K., *Circular Restricted Three-Body Problem*, 2017.

[5] Parker, J. S., and Anderson, R. L., *Low-energy Lunar Trajectory Design*, Jet Propulsion Laboratory, Pasadena, California, 2013.

[6] Davis, K., "Single Shooting Handout," 2017.